


ORIGINAL ARTICLE

Hippocampal Shape Maturation in Childhood and Adolescence

Kirsten M. Lynch ^{1,2}, Yonggang Shi¹, Arthur W. Toga¹ and Kristi A. Clark¹, the Pediatric Imaging, Neurocognition and Genetics Study[†]

¹Keck School of Medicine of USC, USC Mark and Mary Stevens Neuroimaging and Informatics Institute, University of Southern California, Los Angeles, CA 90033, USA and ²Neuroscience Graduate Program, University of Southern California, Los Angeles, CA 90089, USA

Address correspondence to Kristi A. Clark, Laboratory of Neuro Imaging, Mark and Mary Stevens Neuroimaging and Informatics Institute, Keck School of Medicine of USC, 2025 Zonal Ave, Office 213, Los Angeles, CA 90033, USA. Email: kclark@ini.usc.edu

[†]Data used in preparation of this article were obtained from the Pediatric Imaging, Neurocognition and Genetics Study (PING) database (<http://ping.chd.uscd.edu>). As such, the investigators within PING contributed to the design and implementation of PING and/or provided data but did not participate in analysis or writing of this report. A complete listing of PING investigators can be found at <https://ping-dataportal.uscd.edu/sharing/Authors10222012.pdf>.

Abstract

The hippocampus is a subcortical structure critical for learning and memory, and a thorough understanding of its neurodevelopment is important for studying these processes in health and disease. However, few studies have quantified the typical developmental trajectory of the structure in childhood and adolescence. This study examined the cross-sectional age-related changes and sex differences in hippocampal shape in a multisite, multistudy cohort of 1676 typically developing children (age 1–22 years) using a novel intrinsic brain mapping method based on Laplace–Beltrami embedding of surfaces. Significant age-related expansion was observed bilaterally and nonlinear growth was observed primarily in the right head and tail of the hippocampus. Sex differences were also observed bilaterally along the lateral and medial aspects of the surface, with females exhibiting relatively larger surface expansion than males. Additionally, the superior posterior lateral surface of the left hippocampus exhibited an age–sex interaction with females expanding faster than males. Shape analysis provides enhanced sensitivity to regional changes in hippocampal morphology over traditional volumetric approaches and allows for the localization of developmental effects. Our results further support evidence that hippocampal structures follow distinct maturational trajectories that may coincide with the development of learning and memory skills during critical periods of development.

Key words: development, hippocampus, magnetic resonance imaging, morphometry, neuroanatomy

Introduction

The hippocampal formation is a subcortical brain structure within the medial temporal lobe that plays a critical role in diverse learning and memory functions, including episodic memory (Eldridge et al. 2005; Smith and Mizumori 2006), semantic learning (Henke et al. 1999; Manns et al. 2003), and spatial navigation (Maguire et al. 1998; Burgess et al. 2002). The hippocampus also supports broad cognitive processes, such as

attention, perception, and social cognition (Tavares et al. 2015; Aly and Turk-Browne 2017; Mack et al. 2017) and has been implicated in several neurodevelopmental and psychiatric conditions, including schizophrenia (Pujol et al. 2014; Haukvik et al. 2015), major depression (Bijanki et al. 2014; Maller et al. 2017), autism spectrum disorders (Barnea-Goraly et al. 2014; Maier et al. 2015), and anxiety disorders (Machado-de-Sousa et al. 2014; Lindgren et al. 2016). Because many of these

disorders arise during childhood and adolescence (Paus et al. 2008), the study of normative hippocampal development during this period is important to understand atypical development.

The study of human hippocampal development *in vivo* is complicated by the heterogeneous nature of the structure; the hippocampus is composed of several intricate subregions (Duvernoy et al. 2013) and exhibits functional specialization along its long axis (Bannerman et al. 2004; Poppenk et al. 2013; Strange et al. 2014). Hippocampal subregions include the subiculum, cornu ammonis subfields (CA1, CA2, CA3, and CA4), and the dentate gyrus (DG) (Duvernoy et al. 2013). These subregions exhibit distinct cytoarchitectonic features and are differentially associated with distinct aspects of memory formation (Reagh et al. 2014; Stokes et al. 2015; Dimsdale-Zucker et al. 2018; Leal and Yassa 2018). Hippocampal subregions receive its major input from the entorhinal cortex via the perforant pathway (Augustinack et al. 2010; Zeineh et al. 2017) and information subsequently propagates through a series of connections within the hippocampus (Parekh et al. 2015; Zeineh et al. 2017).

The topological and cellular features of the hippocampal subfields are established by birth (Arnold and Trojanowski 1996; Insausti et al. 2010); however, differential patterns of neuronal proliferation, morphological maturation, and myelination occur throughout childhood and adolescence (Seress and Mrzljak 1992; Arnold and Trojanowski 1996; Seress 1998; Lavenex et al. 2007; Lavenex and Banta Lavenex 2013; Dennis et al. 2016). These microstructural changes may be reflected as alterations in regional hippocampal shape or volume during child development.

The functional gradient observed along the anterior–posterior long axis of the hippocampus is reflected by differences in molecular expression (Sun et al. 2015), cell subtype distributions (Ding and Van Hoesen 2015), gene expression (Fanselow and Dong 2010), and connectivity patterns (Poppenk et al. 2013; Reagh and Ranganath 2018). The anterior hippocampus is preferentially involved in anxiety-like behaviors and coarse, global memory representations, while the posterior hippocampus is implicated in spatial learning and fine-grained, local representations (Bannerman et al. 2004; Poppenk and Moscovitch 2011; Strange et al. 2014; Dandolo and Schwabe 2018; Reagh and Ranganath 2018; Sekeres et al. 2018). Previous studies have shown that behavioral performance in these domains are associated with structural and functional differences in the anterior (Rajah et al. 2010; Zeidman et al. 2015) and posterior hippocampi (Maguire et al. 2000, 2006; Keller and Just 2016), which suggests that acquisition and refinement of these behaviors during development may differentially alter hippocampal structure. Because memory function improves rapidly from middle to late childhood (Ghetti and Angelini 2008; Ghetti and Lee 2011; Ofen and Shing 2013), we expect structural hippocampal changes to co-occur during this period.

These maturational changes are commonly explored using whole hippocampal volumetry, however previous studies of normative hippocampal volumetric development yield mixed results; some studies have shown no bilateral age-related change in hippocampal volume (Yurgelun-Todd et al. 2003; Gogtay et al. 2006; Knickmeyer and Gouttard 2008; Lin et al. 2013), while others have found subtle increases in left, right, or bilateral hippocampal volume with age (Giedd et al. 1996; Uematsu et al. 2012; DeMaster et al. 2014). It is likely that volumetric studies may obscure developmentally relevant anatomical changes within specific subregions. Due to the structural and functional heterogeneity observed along the longitudinal and cross-sectional axes, *in vivo* structural MRI approaches measuring regional morphological changes may provide a more complete understanding of hippocampal maturation.

It should be noted that some of the variability seen in previous studies may be due to advances in and availability of MR hardware that influence scan quality. For example, the development and widespread use of multichannel radiofrequency receiver coils over the past decade have resulted in the ability to acquire structural images with increased signal-to-noise ratio and higher spatial resolution compared with single-channel coils (Wiggins et al. 2006), and, when combined with parallel MRI acquisition techniques, significantly reduced acquisition time (Pruessmann et al. 1999; Ji et al. 2007). Now, because these technological advances have become commonplace, researchers are afforded the tissue contrast and spatial resolution necessary in structural MR images to identify subtle changes in hippocampal surface morphology across development.

In contrast to volumetric analyses, shape analysis techniques provide enhanced sensitivity to regionally specific surface deformations that may better reflect local structural changes in development. The global geometry of elongated surfaces, such as the hippocampus, can be quantified with radial distance (RD) measures, which maps the distance from a given vertex to the medial core and is considered a regional index of “thickness” (Thompson et al. 2004; Shi et al. 2009). Global hippocampal shape features may also be a more informative biomarker than volume for memory performance (Voineskos et al. 2015) and heritable traits (Sabuncu et al. 2016).

The first shape analysis studies of hippocampal development reported unique maturational trajectories in individual subregions. Gogtay and colleagues (Gogtay et al. 2006) employed a longitudinal design to explore regional hippocampal changes in a typically developing cohort between 4 and 25 years of age and found differing maturational trajectories along the anterior–posterior axis. While no changes in overall hippocampal volume with age were observed, shape analysis revealed that posterior regions increased with age, while anterior regions decreased with age. Another study, however, found age-related expansion of anterior hippocampal regions in a more restricted age range between 6 and 10 years of age (Lin et al. 2013). These differences could be attributed to different age ranges and small sample sizes. We propose to add to these important findings by capitalizing on a large sample size to provide unprecedented power to detect regional changes in hippocampal morphology over a broad age range.

In this study, we sought to characterize regional hippocampal developmental trajectories and sex differences in a large cross-sectional cohort of 1676 children and adolescents between 1 and 22 years of age using automated volumetric and shape analysis approaches. Localized age and sex effects on intrinsic RD features of the hippocampal surface were explored using the software Metric Optimization for Computational Anatomy (MOCA; https://www.nitrc.org/projects/moca_2015/, 18 September 2018, date last accessed), which provides more accurate anatomical matching because this approach has low edge distortion ratio errors compared with other surface analysis techniques, including spherical demons and unit-sphere projections (Shi, Lai, et al. 2014). Through this framework, we can explore regional hippocampal expansion and deformation in normative development.

Materials and Methods

Subjects and MRI Acquisition

Structural T1-weighted MRI images and demographic data used in the preparation of this article were obtained from three neuroimaging databases of typical child development and combined into a single dataset to increase statistical power to

detect developmental differences. These databases include the Cincinnati MR Imaging of NeuroDevelopment (C-MIND) data repository, the Philadelphia Neurodevelopmental Cohort (PNC) research initiative, and the Pediatric Imaging, Neurocognition and Genetics (PING) Study database.

C-MIND dataset

Cross-sectional neuroimaging data from 80 typically developing participants were considered from the C-MIND study. Structural MRI images were acquired with the same protocol on a 3 T Philips Achieva at Cincinnati Children's Hospital (Holland et al. 2015). All MRI images were manually checked for data quality and scans with excessive motion were discarded. Of the 80 subjects considered, three subjects were excluded due to poor data quality, resulting in 77 C-MIND subjects for the present analysis (40 female, range: 1.4–18.8 years, $M = 9.0$, $SD = 4.5$ years). Demographics of the subjects included is presented in Table 1.

PNC dataset

Structural neuroimaging data from 997 typically developing children and adolescents were acquired by the PNC study at Children's Hospital of Philadelphia (Satterthwaite et al. 2016). Scans were acquired with the same protocol on a 3 T Siemens Tim Trio whole-body MRI. Of the subjects considered for the study, 46 subjects were excluded due to the quality control issues stated above, resulting in 951 PNC subjects in the present analysis (450 female, range: 8.2–22.6 years, $M = 14.8$, $SD = 3.4$ years) (Table 1).

PING dataset

At the time of collection, 801 structural MRI scans were available through the PING database (<http://ping.chd.ucsd.edu/>, 18 September 2018, date last accessed) from a cohort of 695 typically developing children and adolescents. Cross-sectional structural neuroimaging data were acquired from different scanner vendors at nine separate sites (Supplementary Table 1). PING was launched in 2009 by the National Institute on Drug Abuse (NIDA) and the Eunice Kennedy Shriver National Institute of Child Health & Human Development (NICHD) with the primary goal to create a data resource of highly standardized and carefully curated MRI data. Of the 801 scans from the 695 subjects considered for this study, 106 duplicate scans were removed and 47 scans were excluded due to the quality control issues stated above, resulting in the inclusion of 648 cross-sectional scans (309 female, range: 3.2–22.6 years, $M = 11.9$, $SD = 4.9$ years) (Table 1).

In total, 1676 children and adolescents between the ages of 1 and 22 years (mean age \pm standard deviation: 13.4 ± 4.5 years; 850 female) enrolled in C-MIND, PNC, or PING were included in this study (Fig. 1, Table 1). Throughout all protocols, participants had no self-reported history of brain injury or major developmental, psychiatric, or neurological disorders. Across all sites and studies, brain structural imaging was performed using three-dimensional magnetization prepared, rapid-acquisition gradient-echo (MPRAGE) T1-weighted sequences on 3 T MRI scanners with voxel sizes ranging from 0.9375 mm isotropic to $1 \times 1 \times 1.2$ mm³. Scan parameters for each site and study are provided in Supplementary Table 1. Because this study used data from multiple scanners with slightly different spatial resolutions, all neuroimaging data were first resampled to 0.9375 mm isotropic.

Of the 1772 cross-sectional MPRAGE scans considered from the 3 datasets, 29 scans were removed for excessive head

motion, 65 scans were removed for poor hippocampal segmentation, and 2 scans were removed for anatomical abnormalities resulting in the 1676 scans mentioned above.

Image Processing

Across all datasets, image processing consisted of bias-field correction, registration to standard Montreal Neurological Institute (MNI) reference space, brain extraction and tissue-based segmentation using the FSL's anatomical processing pipeline (Smith et al. 2004). Bilateral hippocampal volumes were identified in structural MR images using the FMRIB Software Library (FSL) anatomical processing tool, FIRST (Patenaude et al. 2011). FIRST is a fully automated model-based subcortical segmentation approach that utilizes a multivariate Gaussian framework to extract the most probable volumes from T1-weighted image intensities.

These volumes were then binarized and total hippocampal volume was calculated. In order to normalize for head size, intracranial volume (ICV) was computed per subject in cm³ using the number of voxels contained within the skull. Tissue segmentation in infants is made difficult due to lower signal-to-noise ratio and poor tissue contrast compared with adult MR images (Shi et al. 2010, 2014). Consequently, T1-weighted images alone do not provide effective tissue contrast in infants and segmentation is improved with the addition of T2-weighted images (Williams et al. 2005; Guo et al. 2015). While T2-weighted images were not available in the developmental databases used, steps were taken to ensure the quality of hippocampal segmentations in the infant population analyzed. All T1-weighted images were manually checked for data quality and scans with excessive motion were discarded. Additionally, all segmented hippocampal volumes were visually inspected for anatomical accuracy and only well-delineated structures were considered for analysis. Because tissue contrast in the brain improves after the first year of life, analyses were replicated in a subset that excluded hippocampal segmentations from infants less than 3.17 years of age (see the following).

Hippocampal Mapping/Shape Analysis

Shape analysis was performed using the fully automated Metric Optimization for Computational Anatomy (MOCA) software developed by Shi and colleagues (Shi, Lai, et al. 2014) (Fig. 2). MOCA aligns anatomical features onto brain surfaces using Laplace–Beltrami (LB) eigen functions as isometry-invariant descriptors of surface geometry. Each hippocampal volume was first converted to a triangulated mesh in native space by iteratively updating vertices through outlier detection and surface deformation, resulting in robust topological preservation without shrinkage (Shi, Lai, et al. 2010). In order to probe for inward and outward shape changes, intrinsic local RD measures were determined using the Reeb graph of the first LB eigen function (Shi et al. 2008, 2009). This feature, which reflects local hippocampal thickness, was defined per subject as the shortest distance from each mesh vertex to the long centroidal axis of the hippocampus.

All hippocampal meshes were averaged in a common space to form left- and right-hemisphere hippocampal atlases with 2000 vertices per atlas using SurfStat implemented in Matlab (www.math.mcgill.ca/keith/surfstat, 18 September 2018, date last accessed). The atlas mesh was then projected onto each subject surface using conformal maps, resulting in one-to-one correspondence for statistical analyses.

Table 1 Study demographics by site

Study	Sex	n	ICV (cm ³)				Age (years)				
			Mean	SD	t	P	Mean	SD	Range	t	P
CMN	M	37	1108.4	100.7			10.14	4.48	2.5–17.5		
	F	40	1064.7	113.6	1.78	n.s.	7.93	4.36	1.42–18.83	2.19	*
PNC	M	450	1195.3	104			14.43	3.35	8.25–21.75		
	F	501	1076.6	93.7	18.52	***	15.06	3.44	8.33–22.58	2.85	**
PNG	M	339	1188.5	110.9			11.84	4.86	3.17–21		
	F	309	1067.3	111.6	13.85	***	11.96	5.04	3.17–21	0.31	n.s.
Combined	M	826	1188.6	108.1			13.18	4.32	1.42–22.58		
	F	850	1072.6	101.5	22.63	***	13.6	4.56	2.5–21.75	1.93	n.s.

Note: Statistical tests compare ICV and age with sex (M, male; F, female). Positive t-statistics represent M > F. C-MIND, Cincinnati MR Imaging of NeuroDevelopment dataset; PNC, Philadelphia NeuroDevelopment Cohort; PNG, Pediatric Imaging, Neurocognition and Genetics study; SD, standard deviation; n.s., $P > 0.05$; * $P < 0.05$; ** $P < 0.01$; *** $P < 0.001$.

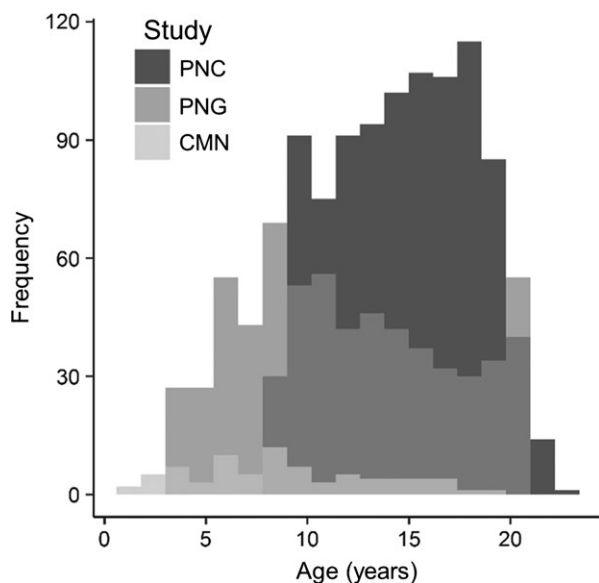


Figure 1. Age distribution of participants included in the present study. The histogram is coded according to study. CMN, Cincinnati MR Imaging of NeuroDevelopment; PNC, Philadelphia Neurodevelopmental Cohort; PNG, Pediatric Imaging, Neurocognition and Genetics study.

Statistical Analysis

All analyses were performed separately on the left and right hippocampi. Because brain size is significantly associated with age and sex during development, ICV was used to calculate the adjusted hippocampal volume, Vol_{adj} (mm³), of each subject using the following equation: $Vol_{adj} = Vol_{raw} * (ICV_m / ICV_i)$, where Vol_{raw} is the raw hippocampal volume, ICV_m is the mean ICV across all subjects, and ICV_i is the individual ICV. This approach allows for hippocampal volumes to be expressed as a proportion of the occupied cranial cavity (Voevodskaya et al. 2014; Nordenskjöld et al. 2015). In order to probe hippocampal anatomical changes that co-occur with intracranial expansion, models without ICV correction were also employed. General linear models (GLMs) were tested for the main effects of age and sex, and age*sex interactions on hippocampal volume. Linear and quadratic age effects were tested on hippocampal volume, and the best fit model was selected using Bayesian information criteria (BIC).

Similar to the volumetric adjustment described above, the per-vertex RD measures obtained with shape analysis were

adjusted for individual head size. For a given vertex i , the adjusted radial distance, $RD_{i,adj}$ (mm), was calculated using the formula: $RD_{i,adj} = RD_{i,raw} * (ICV_m / ICV_i)^{1/3}$, where $RD_{i,raw}$ is the raw radial distance for the i th vertex. Because RD reflects thickness (mm) as opposed to volume (mm³), the ICV adjustment is scaled by the cube root of total brain volume to reflect radial thickness measures as a fraction of the total brain size (Kerchner et al. 2010; Costafreda et al. 2011).

In order to determine regional variability in hippocampal development using shape analysis, GLMs were applied to each adjusted and unadjusted vertex to test for regional effects of age, sex, and age*sex interactions while controlling for scanner type and site. Accordingly, age and sex were included as covariates in order to isolate the specific effects of sex and age, respectively. Quadratic and cubic polynomial models were also explored to identify nonlinear age effects in hippocampal shape. To determine which GLM (linear, quadratic, or cubic polynomial) explains the most age-related variance in RD measures, model selection was performed for each significant vertex using BIC.

Multiple comparison techniques, such as Bonferroni correction, are not appropriate for surface-based analyses because each vertex is not an independent observation—vertices are spatially correlated with their neighbors. Random field theory (RFT) overcomes this by considering both the peaks and spatial extent of smoothed statistical parameter maps using Gaussian random fields (Cao and Worsley 1999; Worsley et al. 1999). The surface topology of highly significant clusters is described by the Euler characteristic, which approximates the corrected P -value at a given cluster level (Friston 1997; Woo et al. 2014). The expected Euler characteristic is derived from the unadjusted P -value and the number of resels, or resolution elements, in the image (Cao and Worsley 1999). This latter property depends on the smoothness of the surface and number of observation points and describes the search volume as a block of vertices with the same size as the image smoothness FWHM (Worsley et al. 1992). A supra-threshold cluster level of $P < 0.001$ and a set level threshold of $P < 0.05$ were specified to determine height and spatial extent thresholds, respectively. Region of interest (ROI) post hoc analyses were then performed on significant age-related clusters to identify the maturational trajectory of developmentally relevant hippocampal regions.

Although all data were resampled to the same resolution, meshes obtained from automatic hippocampal segmentation may be affected by differences in scanner contrast and partial volume effects. To overcome this limitation, all volumetric and surface-based analyses used study and scanner type as covariates, which have been shown to suppress the effects of scanner variability

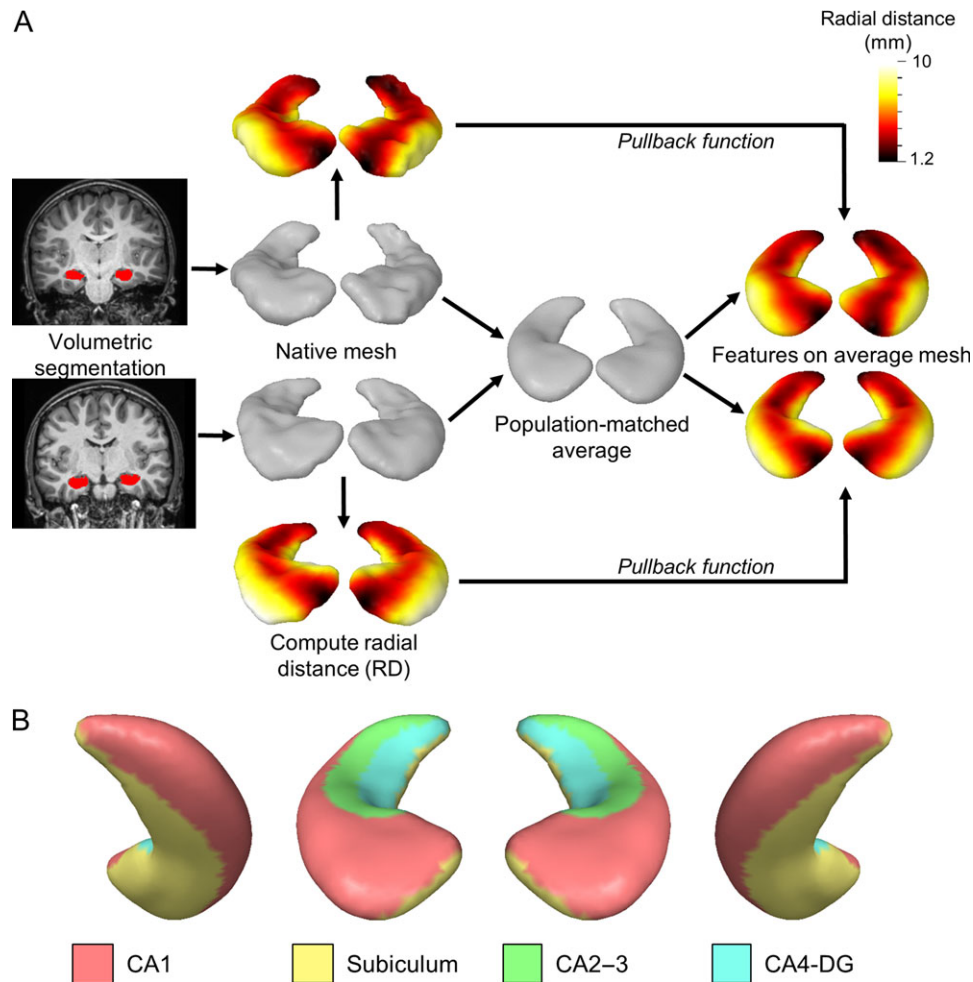


Figure 2. Shape analysis method and hippocampal surface anatomy. (A) Example hippocampal shape analysis procedure from two sample subjects. Hippocampal volumes are segmented from the T1-weighted image using FSL. Each volume surface is converted to a triangulated mesh in native space using MOCA and the RD is computed per vertex. Individual meshes are then averaged together to generate a population-matched average atlas. A pullback function is then applied to project individual RD metrics to the atlas surface to allow for one-to-one correspondence of features. (B) The putative location of subfields are shown on the average hippocampal surface using approximate geometric landmarks from (Winterburn et al. 2013; Iglesias et al. 2015; Yushkevich, Amaral, et al. 2015). From left to right, the right inferior posterior, right superior anterior, left superior anterior, and left inferior posterior surfaces are shown.

(Fennema-Notestine et al. 2007; Pardoe et al. 2008; Chen et al. 2014; Takao et al. 2014). Because all neuroimaging data from subjects younger than 3.17 years were acquired from the same study and scanner (CMN), shape analysis was repeated on a subset of the dataset excluding these 10 infants and toddlers ($N = 1666$) to determine whether this young population biased results (Fig. 1). A marked improvement in T1-weighted tissue contrast is observed in participants greater than 1 year of age (Shi, Yap, et al. 2010; Guo et al. 2015), therefore analyses of this subset were additionally motivated by the effect of tissue contrast on hippocampal segmentation. Analyses were also performed with database-matched age ranges by removing scans acquired from individuals less than 8.25 years of age since the PNC study does not include subjects under this age ($N = 1469$).

Results

Whole-Hippocampus Volumetric Results

Bilateral unadjusted hippocampal volumes exhibited significant nonlinear increases with age as represented with

quadratic polynomials. These increases occurred rapidly in early life and plateaued during adolescence. ICV-adjusted hippocampal volume was also significantly associated with age, left: $b = 0.019$, $t(1675) = 8.02$, $P < 0.001$, adjusted $R^2 = 0.04$; right: $b = 0.019$, $t(1675) = 8.06$, $P < 0.001$, adjusted $R^2 = 0.04$, exhibiting linear volumetric expansion during development with respect to head size (Fig. 3). There was a large effect of hemisphere on adjusted hippocampal volume, $t(1676) = 10.59$, $P < 0.001$, $d = 1.9$, with larger volumes in the right hippocampus ($M = 3.65$, $SD = 0.43$) compared with the left ($M = 3.56$, $SD = 0.44$), and this relationship was maintained for the unadjusted hippocampal volumes.

A medium effect of sex was observed in the unadjusted hippocampal volumes, left: $t(1675) = 8.41$, $P < 0.001$, $d = 0.52$, and right, $t(1675) = 8.53$, $P < 0.001$, $d = 0.51$, with males (left: $M = 3.66$, $SD = 0.46$; right: $M = 3.75$, $SD = 0.47$) having significantly larger hippocampi than females (left: $M = 3.43$, $SD = 0.42$; right: $M = 3.52$, $SD = 0.43$). The nature of this relationship is reversed when adjusting hippocampal volume for ICV (Fig. 3), left: $t(1675) = 6.26$, $P < 0.001$, $d = 0.29$, and right, $t(1675) = 6.73$, $P < 0.001$, $d = 0.33$, with females exhibiting small, but significantly larger

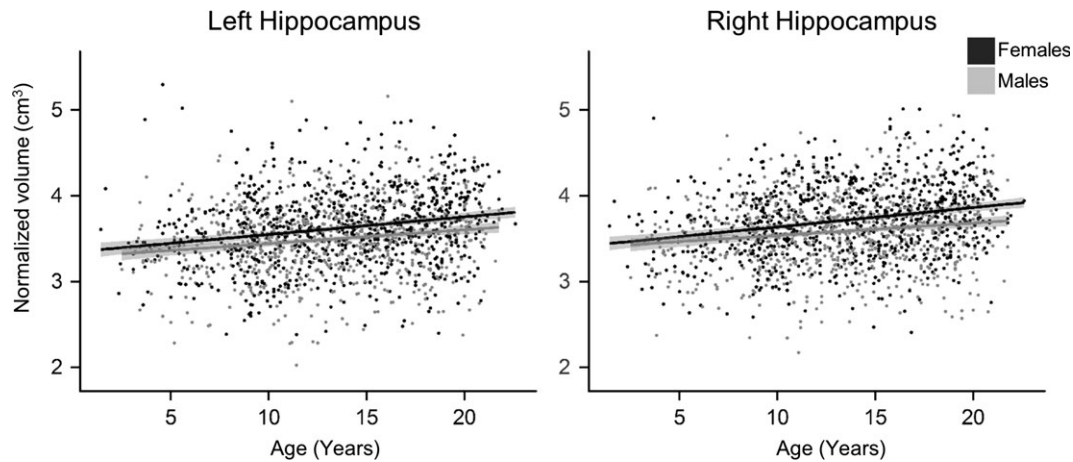


Figure 3. Age-related changes in adjusted hippocampal volume stratified by sex. Bilateral hippocampi adjusted for ICV exhibited sex differences and significant linear volumetric expansion with age when controlling for scanner type and study. Hippocampal volume is represented in cm^3 . Individual data points and regression lines are coded according to sex (gray, males; black, females).

Table 2 Significant clusters related to age and sex using shape analysis

Hemisphere	Test	(x, y, z) Coordinates	Resels	P-value	Direction	
Left	Age	(66.7, 126.9, 58.4)	32.62	<0.001	Linear+	
		(66.0, 125.1, 55.1)	2.12	<0.001	Quadratic+	
		(77.8, 120.6, 62.3)	1.23	<0.001	Quadratic+	
		(65.8, 101.3, 66.9)	0.82	0.005	Quadratic+	
		(69.4, 111.1, 67.4)	0.42	0.03	Quadratic+	
	Sex	(72.1, 106.2, 69.1)	3.64	<0.001	F > M	
		(63.3, 111.1, 61.4)	7.15	<0.001	F > M	
		Age*sex	(63.3, 103.1, 72.3)	0.94	0.002	$F_{\text{rate}} > M_{\text{rate}}$
		(71.6, 122.6, 55.4)	0.41	0.03	$F_{\text{rate}} > M_{\text{rate}}$	
		Right	Age	(116.4, 97.4, 70.7)	32.77	<0.001
(108.7, 115.7, 61.2)	1.29			<0.001	Linear+	
(111.6, 103.8, 71.8)	12.5			<0.001	Quadratic+	
(112.5, 126.5, 53.7)	3.16			<0.001	Quadratic+	
(104.9, 126.2, 58.2)	0.83			0.005	Quadratic-	
Sex	(120.3, 114.7, 68.1)		10.68	<0.001	F > M	
	(109.9, 106.3, 68.9)		6.53	<0.001	F > M	
	(116.4, 126.5, 59.5)		1.23	<0.001	F > M	

Note: Coordinates (x,y,z) correspond to the spatial location of the center of the cluster in Cartesian coordinates on the group-averaged template; resels, resolution elements; +, surface expansion; -, surface contraction; F, female; M, male; F_{rate} and M_{rate} are the slopes obtained by regressing local surface changes on age for females and males, respectively. Adjusted clusterwise P-values from RFT are provided.

proportional hippocampal volumes (left: $M = 3.62$, $SD = 0.44$; right: $M = 3.72$, $SD = 0.43$) than males (left: $M = 3.49$, $SD = 0.43$; right: $M = 3.58$, $SD = 0.42$). Neither adjusted nor unadjusted hippocampal volumes showed age-by-sex interactions.

Age-Related Changes in Hippocampal Shape

Shape analysis results are presented in Table 2. Significant linear and nonlinear age-related expansion (i.e., larger thickness) was observed bilaterally in the unadjusted hippocampal surfaces (not shown). ICV adjustment did not change the maturational pattern of expansion, therefore all results presented here utilized the adjusted hippocampal thickness measures unless otherwise specified. Linear age-related expansion was observed primarily on the superior and inferior surfaces of the hippocampal tail and posterior poles bilaterally. Linear expansion was also observed on the lateral anterior surfaces, bilaterally, and the mesial anterior surface of the left hippocampus (Fig. 4; Table 2)

Quadratic main effect terms in age were also statistically significant in bilateral hippocampal regions, though the effects were more widespread on the right hippocampus where significant quadratic expansion was observed on the lateral surfaces of the hippocampal head and tail (Fig. 4). BIC model selection further supports the use of quadratic age, instead of linear age, when describing developmental shape changes in the right hippocampal tail and head (Fig. 4). While males and females both show statistically significant quadratic age expansion of the right lateral hippocampal head, only females show quadratic age expansion in the right lateral hippocampal tail (Table 3). While no linear age-related decrease in hippocampal thickness was observed bilaterally, a U-shaped quadratic relationship with age was observed in the right medial hippocampal head (Table 2). When stratified by sex, only females show significant inward deformation of the right medial hippocampal head, suggesting that this effect is driven by females (Table 3). Exclusion of participants younger than 3.17 years of age did not

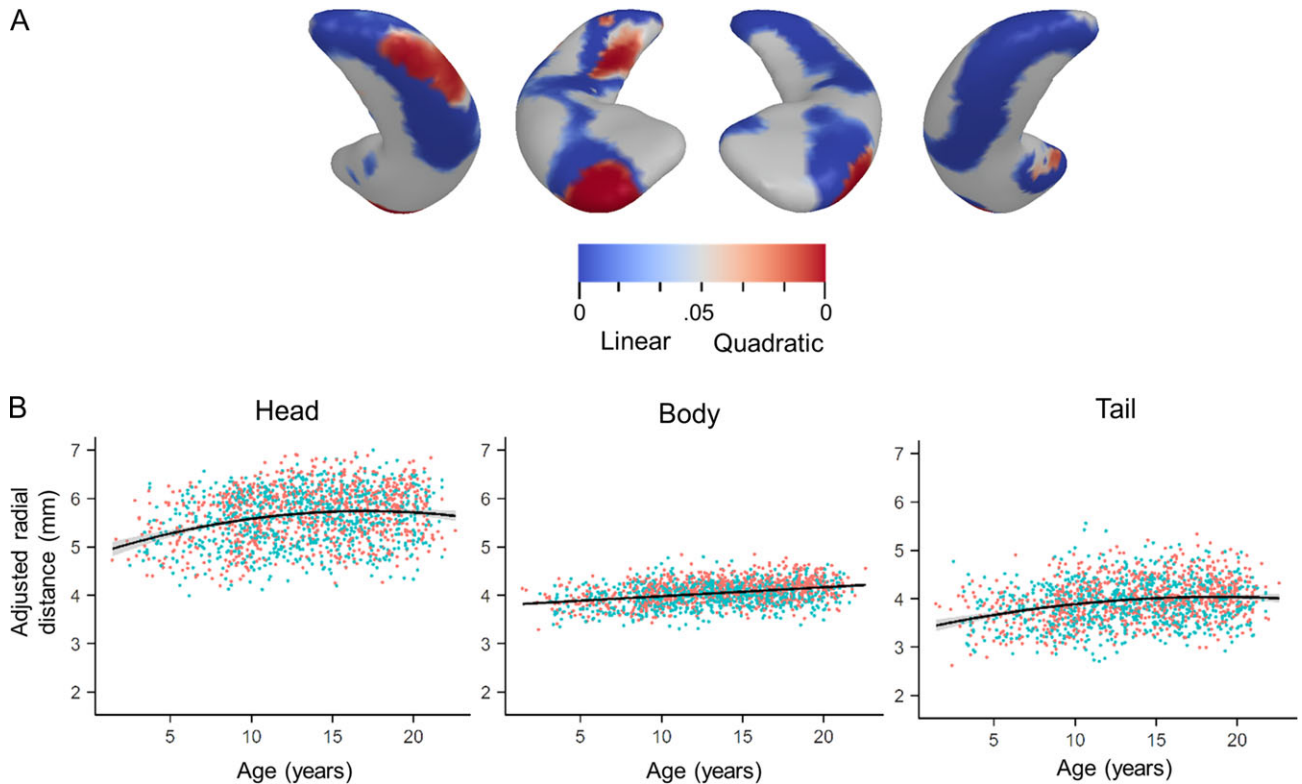


Figure 4. Linear and nonlinear hippocampal expansion with age. (A) P-value maps of linear and quadratic regression of age-related adjusted hippocampal surface expansion using BIC model selection. From left to right, the right inferior posterior, right superior anterior, left superior anterior, and left inferior posterior surfaces are shown. Blue clusters signify linear expansion with age, while red clusters show quadratic expansion with age. Quadratic expansion accounted for more variance than linear expansion primarily on the right hippocampus. All analyses controlled for sex, scanner type, and study. (B) From left to right, ROI analyses for significant age-related clusters on the right hippocampus show quadratic expansion along the lateral head, $y = 5.63 + 4.88x - 2.85x^2$, $P < 0.001$, adjusted $R^2 = 0.060$, linear expansion along the body, $y = 3.79 + 0.019x$, $P < 0.001$, adjusted $R^2 = 0.113$, and quadratic expansion along the tail, $y = 3.94 + 4.22x - 1.75x^2$, $P < 0.001$, adjusted $R^2 = 0.062$.

significantly change the results (Supplementary Fig. 1), however, exclusion of participants younger than 8.25 years of age showed primarily linear age-related expansion in the hippocampal tail and quadratic age effects were not observed.

Hippocampal Shape Sex Differences

Surface-based shape analysis revealed significantly larger surfaces in males along the majority of the left and right unadjusted hippocampal surfaces compared with females, left cluster: 35.2 resels, $t(1674) = 12.39$, $P < 0.001$, $d = 0.61$; right cluster: 32.8 resels, $t(1674) = 10.52$, $P < 0.001$, $d = 0.51$. When adjusting for ICV, the opposite trend was found, though the effect size was smaller (Fig. 5a). Females exhibited significantly larger surfaces compared with males bilaterally along the lateral and medial surfaces of the adjusted hippocampal body (Fig. 5a), accounting for 30% and 37% of the left and right hippocampal surfaces, respectively (Table 2). Neither the left nor right adjusted surfaces displayed significantly larger surfaces in males compared with females. Exclusion of participants younger than 3.17 and 8.25 years of age did not significantly change the results (Supplementary Fig. 2).

Age-Sex Interaction in Hippocampal Shape

A significant interaction between age and sex was observed in the superior posterior lateral body of the left adjusted hippocampus. An ROI analysis of the cluster shows that females exhibit a greater rate of change in surface expansion compared

with males (Fig. 5b). In early childhood, the superior posterior lateral body of the left adjusted hippocampus is larger in males than females; however females surpass males in adjusted size during approximate adolescence. When stratified by sex, this region does not significantly expand with age in males but does in females. No significant age-sex interactions were observed on the right adjusted hippocampus or bilateral unadjusted surfaces. Exclusion of participants younger than 3.17 and 8.25 years of age did not significantly change the results (Supplementary Fig. 3).

The timing and magnitude of left hippocampal shape changes at different developmental time points in males and females are illustrated in Figure 6. Subjects were stratified by sex and binned into age groups (3–5, 9–10, 14–15, and 19–20 years) where the average difference in adjusted hippocampal thickness from baseline (3–5 years) was calculated. In females, left hippocampal head and tail enlargement is apparent by 9–10 years of age, while expansion of the left superior posterior lateral body becomes more apparent in adolescence (14–15 years). Males exhibit modest left hippocampal expansion with age, with growth largely restricted to the head and tail, though to a lesser extent than females.

Discussion

This is the largest study on hippocampal shape analysis in typical development to date, with data from 1676 children and adolescents between the ages of 1 and 22 years of age, allowing for unprecedented power to detect age- and sex-related differences

Table 3 Significant age-related clusters in males and females

Sex	Hemisphere	(x, y, z) Coordinates	Resels	P-value	Direction
Male	Left	(71.2, 98.3, 76.5)	11.58	<0.001	Linear+
		(65.8, 126.3, 58.7)	2.13	<0.001	Linear+
		(78.3, 122.4, 60.1)	1.58	<0.001	Linear+
		(65.4, 125.2, 55.5)	1.34	<0.001	Quadratic+
		(116.5, 98.9, 69.4)	6.71	<0.001	Linear+
	Right	(113.3, 101.7, 73.6)	6.57	<0.001	Linear+
		(114.4, 128.2, 57.6)	2.5	<0.001	Linear+
		(113.7, 128.0, 58.2)	1.22	<0.001	Quadratic+
		(66.7, 126.9, 58.4)	29.06	<0.001	Linear+
		(65.7, 124.3, 55.2)	0.45	0.02	Quadratic+
Females	Left	(116.9, 96.8, 71.2)	30.77	<0.001	Linear+
		(118.5, 97.1, 75.1)	5.14	<0.001	Quadratic+
		(114.2, 125.7, 53.7)	2.56	<0.001	Quadratic+
	Right	(109.1, 121.4, 64.8)	0.71	0.008	Quadratic+
		(104.2, 127.1, 59.1)	0.61	0.01	Quadratic-

Note: Coordinates (x,y,z) correspond to the spatial location of the center of the cluster in Cartesian coordinates on the group-averaged template; resels, resolution elements; +, surface expansion; -, surface contraction; Adjusted clusterwise P-values from RFT are provided.

in regional hippocampal thickness. Bilateral hippocampal volumes increase linearly with age, however hippocampal shape development is heterogeneous and dynamic. Hippocampal subregions follow distinct maturational trajectories with posterior and anterior regions showing nonlinear changes over time primarily in the right hippocampus and the lateral body showing linear expansion bilaterally. Additionally, females showed relatively larger lateral and mesial subregions and more rapid maturation in left posterior regions compared with males.

Although the source of volumetric expansion or contraction is unknown, these changes may reflect differential expression of processes critical for postnatal hippocampal maturation, such as neuronal proliferation, dendritic and axonal elaboration, synaptogenesis, or myelination (Seress and Ribak 1995; Altemus et al. 2005; Lavenex et al. 2007; Insausti et al. 2010; Seress and Ábrahám 2008). Hippocampal structural maturation may also be influenced by neurogenesis, which occurs within the subgranular zone (SGZ) of the postnatal mammalian hippocampus (Kornack and Rakic 1999; Seri et al. 2001; Spalding et al. 2013). While there is evidence that neurogenesis in the SGZ is associated with certain structural and functional features in humans (Hueston et al. 2017; Powell et al. 2017; Toda et al. 2018), recent studies have shown that primate neurogenesis declines rapidly in early childhood (Spalding et al. 2013; Dennis et al. 2016) to undetectable levels by adulthood (Sorrells et al. 2018). Hippocampal expansion during development may also provide more surface area for maturing projections to and from cortical areas to support the acquisition and refinement of hippocampal-dependent behaviors. This relationship between function and shape is supported by evidence showing that hippocampal shape may be a more informative biomarker of working memory performance than subfield volume (Voineskos et al. 2015).

In the present study, age was positively and linearly associated with thickness in superior and inferior lateral posterior hippocampal regions, and these effects persisted when removing subjects less than 8.25 years of age. Nonlinear age-related expansion was observed largely along the right lateral posterior surface. When removing children younger than 8.25 years of age, only the linear age effects in the posterior hippocampus were observed. This suggests developmental expansion of the posterior hippocampus persists through late childhood and

adolescence, which is consistent with rapid improvements in memory performance during this period (Ghetti and Angelini 2008). The developmental expansion in this region appears to correspond to putative CA1 and subiculum subfields. The posterior hippocampus is selectively involved in spatial learning and navigation (Maguire et al. 2000; Keller and Just 2016), perceptual learning (Sheldon and Levine 2016), postencoding processing (Poppenk and Moscovitch 2011), and the representation of fine-grained, local features (Reagh and Ranganath 2018; Sekeres et al. 2018). These perceptual systems depend upon reciprocal connectivity between the posterior two-thirds of the hippocampus and a broader posterior medial network, which includes the cuneus and precuneus, posterior cingulate cortex, parahippocampal cortex, inferior parietal cortex, and retrosplenial cortex (Kahn et al. 2008; Poppenk and Moscovitch 2011; Libby et al. 2012; Reagh and Ranganath 2018; Sekeres et al. 2018). Maturation of these projections may therefore influence the protracted structural development of the posterior hippocampus as reflected by increased thickness and surface area.

The anterior hippocampus exhibited linear age-related expansion of the superior lateral surfaces and nonlinear growth observed on the lateral edges of the hippocampal surface. Interestingly, nonlinear contraction of the surface was observed on the right mesial surface. These regions likely correspond to CA1 and the subiculum, as the subiculum accounts for the largest single cytoarchitectonic field in the hippocampal head (Insausti et al. 2010). The hippocampal head exhibits a different connectivity profile compared with the posterior hippocampus (Poppenk et al. 2013). The anterior hippocampus is functionally correlated with a broader anterior temporal network involved in conceptual processing that includes the amygdala, medial prefrontal cortex, lateral orbitofrontal cortex, and anterior temporopolar cortex (Kahn et al. 2008; Catenoix et al. 2011; Poppenk and Moscovitch 2011; Reagh and Ranganath 2018; Sekeres et al. 2018). In line with this observed connectivity profile, the anterior hippocampus is preferentially involved in anxiety-like behaviors (Satpute et al. 2012; Pantazatos et al. 2014), semantic encoding (Greve et al. 2011), associative learning (Chua et al. 2007; Sheldon and Levine 2016), and processing coarse-grained, global features during memory transformation (Sekeres et al. 2018). The heterogeneous developmental trajectories in the right anterior hippocampus observed in the present study may be attributed to the

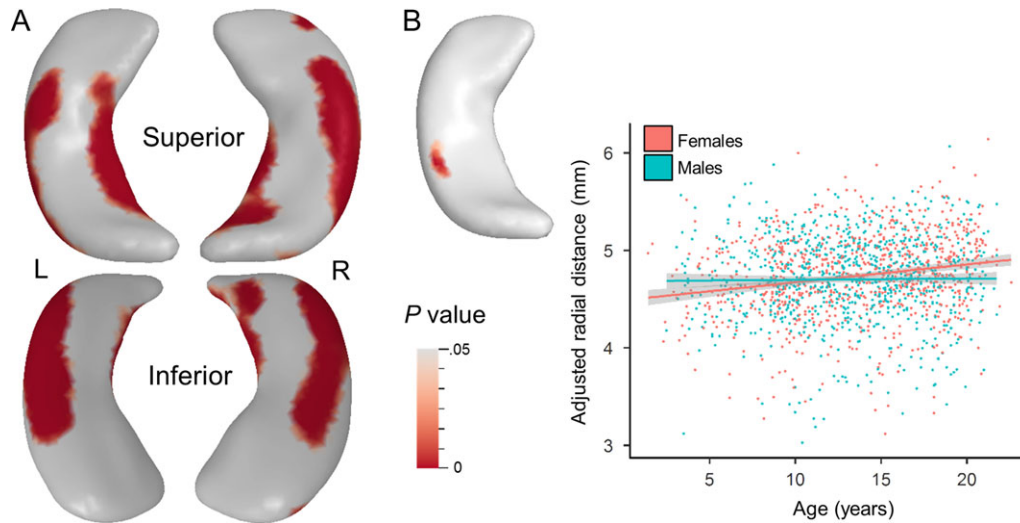


Figure 5. Main effect of sex and age*sex interaction on hippocampal shape. (A) Significant $F > M$ clusters and peaks for the main effect of sex extracted from the t -map using a corrected $P < 0.05$ threshold when controlling for age, scanner type, and study. On the left surface, a cluster on the lateral body, $t(1674) = 8.20$, $P < 0.001$, $d = 0.4$, and mesial body, $t(1674) = 6.12$, $P < 0.001$, $d = 0.3$, reached statistical significance. On the right surface, clusters located on the lateral edge, $t(1674) = 8.68$, $P < 0.001$, $d = 0.42$, medial edge, $t(1674) = 6.76$, $P < 0.001$, $d = 0.33$, and head, $t(1674) = 5.04$, $P < 0.001$, $d = 0.25$, reached significance. (B) Significant age*sex interaction on adjusted hippocampal volume is observed on the superior posterior lateral body of the left hippocampal surface when controlling for scanner type and study. ROI analysis of the significant cluster shows the average adjusted RD regressed against age and stratified by sex. Females show a significant and positive relationship with age, $b = 0.018$, $t(847) = 5.97$, $P < 0.001$, while males do not, $b = 0.0002$, $t(824) = 0.37$, $P = 0.71$. A corrected $P < 0.05$ threshold was applied to obtain the P -value surface maps.

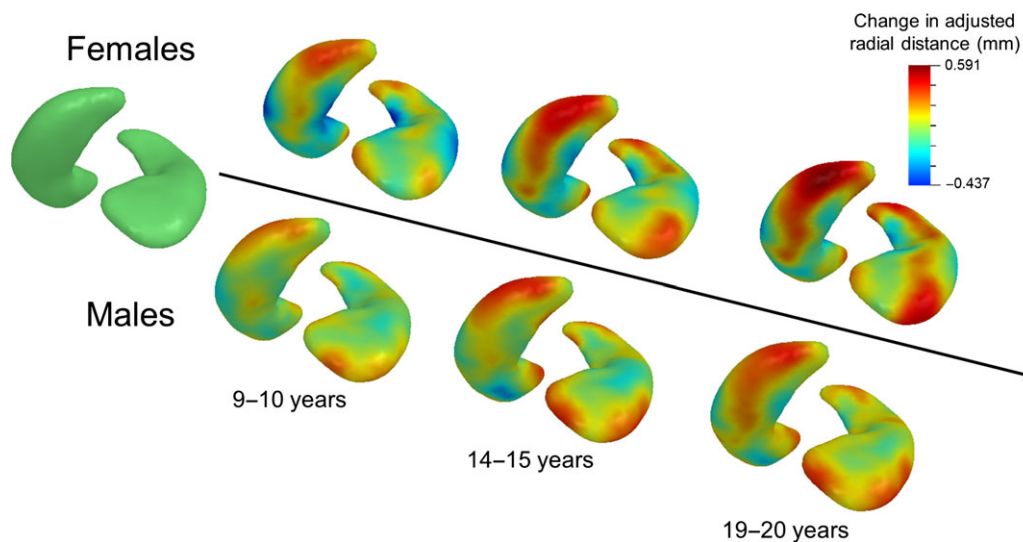


Figure 6. Maturation trajectory of left hippocampal surface in males and females. Data were stratified by sex and split into the following groups: 3–5 years (baseline), 9–10, 14–15, and 19–20 years. For each age group and sex, the inferior posterior surface is presented on the left side and the superior anterior surface is presented on the right side. Adjusted hippocampal surfaces within each age range were averaged together from which the baseline was subtracted to visualize the timing and magnitude of age-related hippocampal surface expansion. Baseline (left-most surface) is illustrated in green. Surface expansion with respect to baseline is mapped in warm colors while surface contract is mapped in cool colors.

diverse functions carried out within the hippocampal head. Additionally, evidence suggests that the functional organization of the hippocampus changes with time (DeMaster et al. 2014; Dandolo and Schwabe 2018). These findings may clarify previous hippocampal shape analysis studies that have found either hippocampal head expansion (Lin et al. 2013) or contraction (Gogtay et al. 2006) during development.

Another explanation for the simultaneous lateral expansion and mesial contraction of the right hippocampal head could be that the anatomical location of the structure physically shifts

during development. Superior and medial to the hippocampal head lies the amygdala (Amunts et al. 2005), which exhibits age-related volumetric expansion when controlling for total brain volume (Østby et al. 2009) and right-greater-than-left structural laterality (Giedd et al. 1996; Uematsu et al. 2012). Therefore, it is possible that the shift in right hippocampal structure occurs via lateral displacement of the hippocampal head by the amygdala during development as they compete for subcortical space. This is supported by evidence that brain structures undergo region-specific maturation resulting in

adult phenotypes that differ slightly in stereotactic location compared to those observed in infants and children (Wilke et al. 2002, 2003; Yoon et al. 2009; Hill et al. 2010).

Overall, we observed that females have larger bilateral hippocampal volumes than males when hippocampal volumes are adjusted for ICV. The present shape analysis results reveal that the observed volumetric differences are localized to the lateral and mesial surfaces of the hippocampal body. Females also exhibited age-related expansion within the superior posterior body of the left hippocampus, while males showed no change in shape (Figs 5 and 6). Previous studies have also reported sex differences in lateral and posterior hippocampal shapes in postpubertal (Neufang et al. 2009; Satterthwaite et al. 2014), but not prepubertal (Satterthwaite et al. 2014) maturation, suggesting that these sex differences do not arise until later in development. Sex differences in hippocampal shape may be attributed to specific cellular mechanisms induced by gonadal hormones (Bramen et al. 2011; Uematsu et al. 2012). Estrogen and androgen epitopes are located throughout the hippocampus, including synapses, dendrites, terminals, and glial cell processes (McEwen and Milner 2007). In animal models, estrogen promotes synaptic plasticity in hippocampal CA1 (Cooke and Woolley 2005; Yuen et al. 2011) and CA3 (Scharfman and MacLusky 2017) pyramidal cells. It has also been shown that estrogen induces neurogenesis within the hippocampal DG SGZ (Bowers et al. 2010) and may play a neuroprotective role (Wise 2006; Bean et al. 2014). The relatively larger surfaces observed in females compared with males in the present study may be due to estrogen-induced synaptogenesis and neural proliferation within the hippocampus. However, the datasets used, with the exception of C-MIND, did not include information on pubertal status or circulating hormone levels, which would have allowed for increased specificity in the identification of the timing and magnitude of sex differences. Therefore, conclusions regarding sex differences related to puberty await further investigation.

The results presented in this current study provide a basis for understanding normative hippocampal development from childhood through adolescence. Our results support the hypothesis that functionally distinct regions within the hippocampus exhibit different developmental trajectories. These maturational changes may co-occur with acquisition of hippocampal-dependent behaviors, however this question was not addressed in the current study. Understanding normative hippocampal development is also important because it provides the basis for identifying deviations from the expected typical developmental trajectory that may be indicative of neurodevelopmental disability. Knowledge of the timing and magnitude of regional hippocampal shape development may help inform the neurobiological underpinnings of disorders associated with hippocampal pathology that arise during childhood and adolescence, including schizophrenia (Paul and Harrison 2004), major depression (Bremner et al. 2000), autism spectrum disorders (Saitoh et al. 2001; Philip et al. 2012), and substance use disorders (Berman et al. 2008). For example, evidence shows inward deformation of the lateral anterior hippocampal head in patients with childhood-onset schizophrenia compared with controls (Johnson et al. 2013), which may map to anterior CA1 subregions (Kalmady et al. 2017). Results from the present study show that this same region exhibits age-related expansion during normative development (Fig. 4), which suggests that patients with childhood-onset schizophrenia may have maturational trajectories that differ from typically developing populations within the anterior head of the hippocampus. Identification of the origin of this deviation in shape may aid in early diagnosis and improved clinical outcomes in patients.

While the present study is the largest study of regional hippocampal development to date and affords power to detect developmental changes and sex differences in a structure as a variable and heterogeneous as the hippocampus, some limitations exist. The study utilized a cross-sectional design; therefore, inferences on individual developmental trajectories cannot be realized without providing longitudinal data points. The scans used in this study were obtained as a part of three separate datasets and acquired on different scanner platforms with slightly different acquisition parameters (Supplementary Table 1), which may have influenced scan quality. While previous studies have shown that differences in scanner version or manufacturer significantly influence gray and white matter contrast ratios in T1-weighted images (Shuter et al. 2008; Shokouhi et al. 2011), the estimated morphometric parameters, such as subcortical volume, do not change significantly across platforms and field strengths in multisite studies (Briellmann et al. 2001; Stonnington et al. 2008; Segall et al. 2009; Jovicich et al. 2009, 2013). Additionally, study and scanner type were used as covariates, which have been shown to suppress the effects of scanner variability (Fennema-Notestine et al. 2007; Pardoe et al. 2008; Chen et al. 2014; Takao et al. 2014). Therefore, we do not suspect that our segmentation process and the resulting shape analysis were compromised by scanner differences.

The age distribution of the sample is highly skewed due to the prevalence of available scans from participants greater than 8 years of age across all databases. We chose to include data from all available ages in order to increase the sensitivity to detect developmental differences; therefore, our results must be interpreted within the constraints of this limitation. Nevertheless, we replicated analyses in subjects greater than 8.25 years of age and found retention of several clusters along the tail that exhibit linear, outward growth over time.

While T1-weighted images provide good subcortical contrast in older children, delineation of the infant hippocampus using structural MRI is challenging because the properties of the developing brain, such as partial myelination, create poor tissue contrast (Shi, Yap, et al. 2010; Shi, Wang, et al. 2014). A multimodal approach to infant hippocampal segmentation utilizing T1- and T2-weighted images would have improved shape analysis results due to the complementary tissue information provided by these contrasts (Williams et al. 2005; Guo et al. 2015), however T2-weighted images were not available from the databases used. To overcome this limitation, all hippocampal segmentations were manually checked for segmentation accuracy and analyses were performed excluding the youngest participants under 3 years of age and discovered the same developmental pattern across the hippocampal surface. Because hippocampal structure changes drastically within the first year of life (Insausti et al. 2010), future studies should seek to understand how hippocampal shape changes during infancy utilizing methods more precisely tailored to the unique challenges that come with segmenting developing neonatal tissue (Shi, Fan, et al. 2010; Shi, Yap, et al. 2010; Shi, Wang, et al. 2014).

Shape analysis is sensitive to structural changes, however it does not provide specific information regarding the nature of these changes. Because shape analysis techniques only consider intrinsic surface features, differences in shape may reflect a number of structural phenomena within the sampled space. Therefore, significant developmental differences at a given vertex cannot be uniquely attributed to a specific subfield. The development of new hippocampal segmentation techniques for structural MRI allows for subfield specificity (Winterburn et al.

2013; Iglesias et al. 2015; Yushkevich, Pluta, et al. 2015); however these approaches may not provide sufficient accuracy due to technical limitations on the spatial resolution required to resolve individual subfield boundaries in clinically feasible scans (Amunts et al. 2005; Wisse et al. 2012; Winterburn et al. 2013). Recent technological advances, including the increased availability of ultrahigh-field MRI (Giuliano et al. 2017) and parallel imaging techniques utilizing multichannel receiver coils, such as simultaneous multislice imaging techniques (Barth et al. 2016; Setsompop et al. 2016), provide submillimeter resolution at reduced acquisition times to enable detailed subfield morphology (Giuliano et al. 2017). Future studies should aim to characterize how changes in individual subfield volumes and morphometry influence regional features on the surface of the hippocampus in order to better understand the underlying neurobiological changes in hippocampal shape that occur during child and adolescent development.

The current study supports previous findings in hippocampal development showing relatively larger bilateral hippocampal volumes in females compared with males and significant age-related volumetric growth. The findings also provide novel evidence identifying hippocampal regions that contribute to these overall differences. Specifically, age-related volumetric enlargement of the hippocampus is accompanied by global linear surface expansion in the left and right hippocampi, and nonlinear expansion of the head and tail primarily in the right hippocampal surface. The larger adjusted hippocampal volumes in females may be localized to the lateral and mesial surfaces bilaterally and could be further exaggerated by the faster maturation of the left lateral surface observed in females compared with males. Results from this large, multisite study across infancy and early adulthood contributes to a growing compendium of evidence describing dynamic developmental trajectories in structural hippocampal maturation that are characterized by a complex interplay between age and sex. Future studies should aim to correlate changes in memory with hippocampal shape in development to determine how functional modification is reflected in structure.

Supplementary Material

Supplementary material is available at *Cerebral Cortex* online.

Funding

The Eunice Kennedy Shriver National Institute of Child Health and Human Development (R00HD065832), the National Institute of Biomedical Imaging and Bioengineering (P41EB015922 and U54EB020406), the National Institute of Neurological Disorders and Stroke (R21NS091586), and the National Institute of Mental Health (R01MH094343) and partially support from NARSAD Young Investigator Award. Data collection and sharing for this project was funded by the Philadelphia Neurodevelopmental Cohort (PNC) (Supported by RC2 grants from the National Institute of Mental Health, MH089983 and MH089924, as well as T32MH019112), The Cincinnati MR Imaging of Neurodevelopment study (C-MIND) (supported by the National Institute of Child Health and Human Development Grant HHSN275200900018C) and the Pediatric Imaging, Neurocognition and Genetics Study (PING) (National Institutes of Health Grant RC2DA029475). PING is funded by the National Institute on Drug Abuse and the Eunice Kennedy Shriver National Institute of Child Health & Human Development. PING data are disseminated by the PING

Coordinating Center at the Center for Human Development, University of California, San Diego.

Notes

The authors would like to thank Lu Zhao, Ryan Cabeen, Farshid Sepehrband, and Megan Herting for their comments, support, and assistance navigating MOCA tools. *Conflict of Interest:* None declared.

References

- Altemus KL, Lavenex P, Ishizuka N, Amaral DG. 2005. Morphological characteristics and electrophysiological properties of CA1 pyramidal neurons in macaque monkeys. *Neuroscience*. 136:741–756.
- Aly M, Turk-Browne NB. 2017. Flexible weighting of diverse inputs makes hippocampal function malleable. *Neurosci Lett* 680:13–22.
- Amunts K, Kedo O, Kindler M, Pieperhoff P, Mohlberg H, Shah NJ, Habel U, Schneider F, Zilles K. 2005. Cytoarchitectonic mapping of the human amygdala, hippocampal region and entorhinal cortex: Intersubject variability and probability maps. *Anat Embryol (Berl)*. 210:343–352.
- Arnold SE, Trojanowski JQ. 1996. Human fetal hippocampal development: and neuronal morphologic features. *J Comp Neurol*. 367:274–292.
- Augustinack JC, Helmer K, Huber KE, Kakunoori S, Zöllei L, Fischl B, Kroenke C, Health O. 2010. Direct visualization of the perforant pathway in the human brain with ex vivo diffusion tensor imaging. *Front Hum Neurosci*. 4:1–13.
- Bannerman DM, Rawlins JNP, McHugh SB, Deacon RMJ, Yee BK, Bast T, Zhang WN, Pothuisen HHJ, Feldon J. 2004. Regional dissociations within the hippocampus—memory and anxiety. *Neurosci Biobehav Rev*. 28:273–283.
- Barnea-Goraly N, Frazier TW, Piacenza L, Minshew NJ, Keshavan MS, Reiss AL, Hardan AY. 2014. A preliminary longitudinal volumetric MRI study of amygdala and hippocampal volumes in autism. *Prog Neuropsychopharmacol Biol Psychiatry*. 48:124–128.
- Barth M, Breuer F, Koopmans PJ, Norris DG, Poser BA. 2016. Simultaneous multislice (SMS) imaging techniques. *Magn Reson Med*. 75:63–81.
- Bean LA, Ianov L, Foster TC. 2014. Estrogen receptors, the hippocampus, and memory. *Neuroscientist*. 20:534–545.
- Berman S, O'Neill J, Fears S, Bartzokis G, London ED. 2008. Abuse of amphetamines and structural abnormalities in the brain. *Ann N Y Acad Sci*. 1141:195–220.
- Bijanki KR, Hodis B, Brumm MC, Harlynn EL, McCormick LM. 2014. Hippocampal and left subcallosal anterior cingulate atrophy in psychotic depression. *PLoS One*. 9:1–7.
- Bowers JM, Waddell J, McCarthy MM. 2010. A developmental sex difference in hippocampal neurogenesis is mediated by endogenous oestradiol. *Biol Sex Differ*. 1:8.
- Bramen JE, Hranilovich JA, Dahl RE, Forbes EE, Chen J, Toga AW, Dinov ID, Worthman CM, Sowell ER. 2011. Puberty influences medial temporal lobe and cortical gray matter maturation differently in boys than girls matched for sexual maturity. *Cereb Cortex*. 21:636–646.
- Bremner JD, Narayan M, Anderson ER, Staib LH, Miller HL, Charney DS. 2000. Hippocampal volume reduction in major depression. *Am J Psychiatry*. 157:115–118.
- Briellmann RS, Syngienotis A, Jackson GD. 2001. Comparison of hippocampal volumetry at 1.5 tesla and at 3 tesla. *Epilepsia*. 42:1021–1024.

- Burgess N, Maguire EA, O'Keefe J. 2002. The human hippocampus and spatial and episodic memory. *Neuron*. 35:625–641.
- Cao J, Worsley KJ. 1999. The detection of local shape changes via the geometry of Hotelling's T₂ fields. *Ann Stat*. 27:925–942.
- Catenoix H, Magnin M, Mauguière F, Ryvlin P. 2011. Evoked potential study of hippocampal efferent projections in the human brain. *Clin Neurophysiol*. 122:2488–2497.
- Chen J, Liu J, Calhoun VD, Arias-Vasquez A, Zwiers MP, Gupta CN, Franke B, Turner JA. 2014. Exploration of scanning effects in multi-site structural MRI studies. *J Neurosci Methods*. 230:37–50.
- Chua EF, Schacter DL, Rand-Giovannetti E, Sperling RA. 2007. Evidence for a specific role of the anterior hippocampal region in successful associative encoding. *Hippocampus*. 17:1071–1080.
- Cooke BM, Woolley CS. 2005. Gonadal hormone modulation of dendrites in the mammalian CNS. *J Neurobiol*. 64:34–46.
- Costafreda SG, Dinov ID, Tu Z, Shi Y, Liu CY, Kloszewska I, Mecocci P, Soininen H, Tsolaki M, Vellas B, et al. 2011. Automated hippocampal shape analysis predicts the onset of dementia in mild cognitive impairment. *Neuroimage*. 56:212–219.
- Dandolo LC, Schwabe L. 2018. Time-dependent memory transformation along the hippocampal anterior–posterior axis. *Nat Commun*. 9:1205.
- DeMaster D, Pathman T, Lee JK, Ghetti S. 2014. Structural development of the hippocampus and episodic memory: developmental differences along the anterior/posterior axis. *Cereb Cortex*. 24:3036–3045.
- Dennis CV, Suh LS, Rodriguez ML, Kril JJ, Sutherland GT. 2016. Human adult neurogenesis across the ages: an immunohistochemical study. *Neuropathol Appl Neurobiol*. 42:621–638.
- Dimsdale-Zucker HR, Ritchey M, Ekstrom AD, Yonelinas AP, Ranganath C. 2018. CA1 and CA3 differentially support spontaneous retrieval of episodic contexts within human hippocampal subfields. *Nat Commun*. 9:294.
- Ding SL, Van Hoesen GW. 2015. Organization and detailed parcellation of human hippocampal head and body regions based on a combined analysis of Cyto- and chemoarchitecture. *J Comp Neurol*. 523:2233–2253.
- Duvernoy H, Cattin F, Risold P-Y. 2013. *The Human Hippocampus: Functional anatomy, vascularization and serial sections with MRI*. 4th ed. Berlin, Germany: Springer.
- Eldridge LL, Engel SA, Zeineh MM, Bookheimer SY, Knowlton BJ. 2005. A dissociation of encoding and retrieval processes in the human hippocampus. *J Neurosci*. 25:3280–3286.
- Fanselow MS, Dong HW. 2010. Are the dorsal and ventral hippocampus functionally distinct structures? *Neuron*. 65:7–19.
- Fennema-Notestine C, Gamst AC, Quinn BT, Pacheco J, Jernigan TL, Thal L, Buckner R, Killiany R, Blacker D, Dale AM, et al. 2007. Feasibility of multi-site clinical structural neuroimaging studies of aging using legacy data. *Neuroinformatics*. 5:235–245.
- Friston KJ. 1997. Testing for anatomically specified regional effects. *Hum Brain Mapp*. 5:133–136.
- Ghetti S, Angelini L. 2008. The development of recollection and familiarity in childhood and adolescence: evidence from the dual-process signal detection model. *Child Dev*. 79:339–358.
- Ghetti S, Lee J. 2011. *Children's episodic memory*. Wiley Interdiscip Rev Cogn Sci. 2:365–373.
- Giedd J, Vaituzis C, Hamburger S, Lange N, Rajapakse JC, Kaysen D, Vauss YC, Rapoport JL. 1996. Quantitative MRI of the temporal lobe, amygdala, and hippocampus in normal human development: ages 4–18 years. *J Comp Neurol*. 366:223–230.
- Giuliano A, Donatelli G, Cosottini M, Tosetti M, Retico A, Fantacci ME. 2017. Hippocampal subfields at ultra high field MRI: an overview of segmentation and measurement methods. *Hippocampus*. 27:481–494.
- Gogtay N, Nugent TF, Herman DH, Ordonez A, Greenstein D, Hyashi KM, Clasen L, Toga AW, Giedd JN, Rapoport JL, et al. 2006. Dynamic mapping of normal human hippocampal development. *Hippocampus*. 16:664–672.
- Greve A, Evans CJ, Graham KS, Wilding EL. 2011. Functional specialisation in the hippocampus and perirhinal cortex during the encoding of verbal associations. *Neuropsychologia*. 49:2746–2754.
- Guo Y, Wu G, Yap P-T, Jewells V, Lin W, Shen D. 2015. Segmentation of infant hippocampus using common feature representations learned for multimodal longitudinal data. *Med Image Comput Comput Assist Interv*. 9351:63–71.
- Haukvik UK, Westlye LT, Mørch-Johnsen L, Jørgensen KN, Lange EH, Dale AM, Melle I, Andreassen OA, Agartz I. 2015. In vivo hippocampal subfield volumes in schizophrenia and bipolar disorder. *Biol Psychiatry*. 77:581–588.
- Henke K, Weber B, Kneifel S, Wieser HG, Buck A. 1999. Human hippocampus associates information in memory. *Proc Natl Acad Sci USA*. 96:5884–5889.
- Hill J, Inder T, Neil J, Dierker D, Harwell J, Van Essen D. 2010. Similar patterns of cortical expansion during human development and evolution. *Proc Natl Acad Sci USA*. 107:13135–13140.
- Holland S, Schmithorst VJ, Wagner M, Lee G, Rajagopal A, Sroka M, Felicelli N, Rupert A, Clark K, Toga A, et al. 2015. The C-MIND project: normative MRI and behavioral data from children from birth to 18 years. In: *Proceedings of the 21st Annual Meeting of the Organization for Human Brain Mapping (OHBM)*, Honolulu, HA.
- Hueston CM, Cryan JF, Nolan YM. 2017. Stress and adolescent hippocampal neurogenesis: diet and exercise as cognitive modulators. *Transl Psychiatry*. 7:e1081–17.
- Iglesias JE, Augustinack JC, Nguyen K, Player CM, Player A, Wright M, Roy N, Frosch MP, McKee AC, Wald LL, et al. 2015. A computational atlas of the hippocampal formation using ex vivo, ultra-high resolution MRI: application to adaptive segmentation of in vivo MRI. *Neuroimage*. 115:117–137.
- Insausti R, Cebada-Sánchez S, Marcos P. 2010. Postnatal development of the human hippocampal formation. *Adv Anat Embryol Cell Biol*. 206:1–86.
- Ji JX, Son JB, Rane SD. 2007. PULSAR: a MATLAB toolbox for parallel magnetic resonance imaging using array coils and multiple channel receivers. *Concepts Magn Reson Part B Magn Reson Eng*. 31B:24–36.
- Johnson SLM, Wang L, Alpert KI, Greenstein D, Clasen L, Lalonde F, Miller R, Rapoport J, Gogtay N. 2013. Hippocampal shape abnormalities of patients with childhood-onset schizophrenia and their unaffected siblings. *J Am Acad Child Adolesc Psychiatry*. 52:527–536.
- Jovicich J, Czanner S, Han X, Salat D, van der Kouwe A, Quinn B, Pacheco J, Albert M, Killiany R, Blacker D, et al. 2009. MRI-derived measurements of human subcortical, ventricular and intracranial brain volumes: reliability effects of scan sessions, acquisition sequences, data analyses, scanner upgrade, scanner vendors and field strengths. *Neuroimage*. 46:177–192.
- Jovicich J, Marizzoni M, Sala-Llonch R, Bosch B, Bartrés-Faz D, Arnold J, Benninghoff J, Wiltfang J, Roccatagliata L, Nobili F,

- et al. 2013. Brain morphometry reproducibility in multi-center 3T MRI studies: a comparison of cross-sectional and longitudinal segmentations. *Neuroimage*. 83:472–484.
- Kahn I, Andrews-Hanna JR, Vincent JL, Snyder AZ, Buckner RL. 2008. Distinct cortical anatomy linked to subregions of the medial temporal lobe revealed by intrinsic functional connectivity. *J Neurophysiol*. 100:129–139.
- Kalmady SV, Shivakumar V, Arasappa R, Subramaniam A, Gautham S, Venkatasubramanian G, Gangadhar BN. 2017. Clinical correlates of hippocampus volume and shape in anti-psychotic-naïve schizophrenia. *Psychiatry Res - Neuroimaging*. 263:93–102.
- Keller TA, Just MA. 2016. NeuroImage structural and functional neuroplasticity in human learning of spatial routes. *Neuroimage*. 125:256–266.
- Kerchner GA, Hess CP, Hammond-Rosenbluth KE, Xu D, Rabinovici GD, Kelley DAC, Vigneron DB, Nelson SJ, Miller BL. 2010. Hippocampal CA1 apical neuropil atrophy in mild Alzheimer disease visualized with 7-T MRI. *Neurology*. 75:1381–1387.
- Knickmeyer R, Gouttard S. 2008. A structural MRI study of human brain development from birth to 2 years. *J Neurosci*. 28:12176–12182.
- Kornack DR, Rakic P. 1999. Continuation of neurogenesis in the hippocampus of the adult macaque monkey. *Proc Natl Acad Sci USA*. 96:5768–5773.
- Lavenex P, Banta Lavenex P. 2013. Building hippocampal circuits to learn and remember: insights into the development of human memory. *Behav Brain Res*. 254:8–21.
- Lavenex P, Banta Lavenex P, Amaral DG. 2007. Postnatal development of the primate hippocampal formation. *Dev Neurosci*. 29:179–192.
- Leal SL, Yassa MA. 2018. Integrating new findings and examining clinical applications of pattern separation. *Nat Neurosci*. 21:163–173.
- Libby LA, Ekstrom AD, Ragland JD, Ranganath C. 2012. Differential connectivity of perirhinal and parahippocampal cortices within human hippocampal subregions revealed by high-resolution functional imaging. *J Neurosci*. 32:6550–6560.
- Lin M, Fwu PT, Buss C, Davis EP, Head K, Muftuler LT, Sandman CA, Su M-Y. 2013. Developmental changes in hippocampal shape among preadolescent children. *Int J Dev Neurosci*. 31:473–481.
- Lindgren L, Bergdahl J, Nyberg L. 2016. Longitudinal evidence for smaller hippocampus volume as a vulnerability factor for perceived stress. *Cereb Cortex*. 26:3527–3533.
- Machado-de-Sousa JP, De Lima Osório F, Jackowski AP, Bressan RA, Chagas MHN, Torro-Alves N, DePaula ALD, Crippa JAS, Hallak JEC. 2014. Increased amygdalar and hippocampal volumes in young adults with social anxiety. *PLoS One*. 9:1–5.
- Mack ML, Love BC, Preston AR. 2017. Building concepts one episode at a time: The hippocampus and concept formation. *Neurosci Lett*. 680:31–38.
- Maguire EA, Burgess N, Donnett JG, Frackowiak RSJ, Frith CD, Okeefe J. 1998. Knowing where and getting there. *Science*. 280:921–924.
- Maguire EA, Gadian DG, Johnsrude IS, Good CD, Ashburner J, Frackowiak RSJ, Frith CD. 2000. Navigation-related structural change in the hippocampi of taxi drivers. *Proc Natl Acad Sci*. 97:4398–4403.
- Maguire EA, Woollett K, Spiers HJ. 2006. London taxi drivers and bus drivers: a structural MRI and neuropsychological analysis. *Hippocampus*. 16:1091–1101.
- Maier S, Tebartz van Elst L, Beier D, Ebert D, Fangmeier T, Radtke M, Perlov E, Riedel A. 2015. Increased hippocampal volumes in adults with high functioning autism spectrum disorder and an IQ>100: a manual morphometric study. *Psychiatry Res - Neuroimaging*. 234:152–155.
- Maller JJ, Broadhouse K, Rush AJ, Gordon E, Koslow S, Grieve SM. 2017. Increased hippocampal tail volume predicts depression status and remission to anti-depressant medications in major depression. *Mol Psychiatry*. doi:10.1038/mp.2017.224.
- Manns JR, Hopkins RO, Squire LR. 2003. Semantic memory and the human hippocampus. *Neuron*. 38:127–133.
- McEwen BS, Milner TA. 2007. Hippocampal formation: shedding light on the influence of sex and stress on the brain. *Brain Res Rev*. 55:343–355.
- Neufang S, Specht K, Hausmann M, Güntürkün O, Herpertz-Dahlmann B, Fink GR, Konrad K. 2009. Sex differences and the impact of steroid hormones on the developing human brain. *Cereb Cortex*. 19:464–473.
- Nordenskjöld R, Malmberg F, Larsson EM, Simmons A, Ahlström H, Johansson L, Kullberg J. 2015. Intracranial volume normalization methods: considerations when investigating gender differences in regional brain volume. *Psychiatry Res-Neuroimaging*. 231:227–235.
- Ofen N, Shing YL. 2013. From perception to memory: changes in memory systems across the lifespan. *Neurosci Biobehav Rev*. 37:2258–2267.
- Pantazatos SP, Talati A, Schneier FR, Hirsch J. 2014. Reduced anterior temporal and hippocampal functional connectivity during face processing discriminates individuals with social anxiety disorder from healthy controls and panic disorder, and increases following treatment. *Neuropsychopharmacology*. 39:425–434.
- Pardoe H, Pell GS, Abbott DF, Berg AT, Jackson GD. 2008. Multi-site voxel-based morphometry: methods and a feasibility demonstration with childhood absence epilepsy. *Neuroimage*. 42:611–616.
- Parekh MB, Rutt BK, Purcell R, Chen Y, Zeineh MM. 2015. Ultra-high resolution in-vivo 7.0 T structural imaging of the human hippocampus reveals the endfolial pathway. *Neuroimage*. 112:1–6.
- Patenaude B, Smith SM, Kennedy DN, Jenkinson M. 2011. A Bayesian model of shape and appearance for subcortical brain segmentation. *Neuroimage*. 56:907–922.
- Paul EW, Harrison J. 2004. The hippocampus in schizophrenia: a review of the neuropathological evidence and its pathophysiological implications. *Psychopharmacology (Berl)*. 174:151–162.
- Paus T, Keshavan M, Giedd JN. 2008. Why do many psychiatric disorders emerge during adolescence? *Nat Rev Neurosci*. 9:947–957.
- Philip RCM, Dauvermann MR, Whalley HC, Baynham K, Lawrie SM, Stanfield AC. 2012. A systematic review and meta-analysis of the fMRI investigation of autism spectrum disorders. *Neurosci Biobehav Rev*. 36:901–942.
- Poppenk J, Evensmoen HR, Moscovitch M, Nadel L. 2013. Long-axis specialization of the human hippocampus. *Trends Cogn Sci*. 17:230–240.
- Poppenk J, Moscovitch M. 2011. A hippocampal marker of recollection memory ability among healthy young adults: contributions of posterior and anterior segments. *Neuron*. 72:931–937.
- Powell TR, Murphy T, Lee SH, Duarte RRR, Lee HA, Smeeth D, Price J, Breen G, Thuret S. 2017. Inter-individual variation in genes governing human hippocampal progenitor differentiation

- in vitro is associated with hippocampal volume in adulthood. *Sci Rep.* 7:15112.
- Pruessmann KP, Weiger M, Scheidegger MB, Boesiger P. 1999. SENSE: sensitivity encoding for fast MRI. *Magn Reson Med.* 42:952–962.
- Pujol N, Penadés R, Junqué C, Dinov I, Fu CHY, Catalán R, Ibarretxe-Bilbao N, Bargalló N, Bernardo M, Toga A, et al. 2014. Hippocampal abnormalities and age in chronic schizophrenia: morphometric study across the adult lifespan. *Br J Psychiatry.* 205:369–375.
- Rajah MN, Kromas M, Han JE, Pruessner JC. 2010. Group differences in anterior hippocampal volume and in the retrieval of spatial and temporal context memory in healthy young versus older adults. *Neuropsychologia.* 48:4020–4030.
- Reagh ZM, Ranganath C. 2018. What does the functional organization of cortico-hippocampal networks tell us about the functional organization of memory? *Neurosci Lett.* 680:69–76.
- Reagh ZM, Watabe J, Ly M, Murray E, Yassa MA. 2014. Dissociated signals in human dentate gyrus and CA3 predict different facets of recognition memory. *J Neurosci.* 34:13301–13313.
- Sabuncu MR, Ge T, Holmes AJ, Smoller JW, Buckner RL, Fischl B, Alzheimer's Disease Neuroimaging Initiative the ADN. 2016. Morphometricity as a measure of the neuroanatomical signature of a trait. *Proc Natl Acad Sci USA.* 113:E5749–E5756.
- Saitoh O, Karns CM, Courchesne E. 2001. Development of the hippocampal formation from 2 to 42 years: MRI evidence of smaller area dentata in autism. *Brain.* 124:1317–1324.
- Satpute AB, Mumford JA, Naliboff BD, Poldrack RA. 2012. Human anterior and posterior hippocampus respond distinctly to state and trait anxiety. *Emotion.* 12:58–68.
- Satterthwaite TD, Connolly JJ, Ruparel K, Calkins ME, Jackson C, Elliott MA, Roalf DR, Hopsona R, Prabhakaran K, Behr M, et al. 2016. The Philadelphia neurodevelopmental cohort: a publicly available resource for the study of normal and abnormal brain development in youth. *Neuroimage.* 124:1115–1119.
- Satterthwaite TD, Vandekar S, Wolf DH, Ruparel K, Roalf DR, Jackson C, Elliott MA, Bilker WB, Calkins ME, Prabhakaran K, et al. 2014. Sex differences in the effect of puberty on hippocampal morphology. *J Am Acad Child Adolesc Psychiatry.* 53:341–350.
- Scharfman HE, MacLusky NJ. 2017. Sex differences in hippocampal area CA3 pyramidal cells. *J Neurosci Res.* 95:563–575.
- Segall JM, Turner JA, Van Erp TGM, White T, Bockholt HJ, Gollub RL, Ho BC, Magnotta V, Jung RE, McCarley RW, et al. 2009. Voxel-based morphometric multisite collaborative study on schizophrenia. *Schizophr Bull.* 35:82–95.
- Sekeres MJ, Winocur G, Moscovitch M. 2018. The hippocampus and related neocortical structures in memory transformation. *Neurosci Lett.* 680:39–53.
- Seress L. 1998. Neuronal connections, cell formation and cell migration in the perinatal human hippocampal dentate gyrus. *Cesk Fysiol.* 47:42–50.
- Seress L, Mrzljak L. 1992. Postnatal development of mossy cells in the human dentate gyrus: A light microscopic Golgi study. *Hippocampus.* 2:127–141.
- Seress L, Ribak CE. 1995. Postnatal-development of CA3 pyramidal neurons and their afferents in the ammons horn of rhesus-monkeys. *Hippocampus.* 5:217–231.
- Seress L, Abraham H. 2008. Pre- and postnatal morphological development of the human hippocampal formation. In: Nelson CA, Luciana M, editors. *Handbook of Developmental Cognitive Neuroscience.* 2nd ed. Cambridge, MA: MIT Press. p. 187–211.
- Seri B, Garcia-Verdugo JM, McEwen BS, Alvarez-Buylla A. 2001. Astrocytes give rise to new neurons in the adult mammalian hippocampus. *J Neurosci.* 21:7153–7160.
- Setsompop K, Feinberg DA, Polimeni JR. 2016. Rapid brain MRI acquisition techniques at ultra-high fields. *NMR Biomed.* 29:1198–1221.
- Sheldon S, Levine B. 2016. The role of the hippocampus in memory and mental construction. *Ann N Y Acad Sci.* 1369:76–92.
- Shi F, Fan Y, Tang S, Gilmore JH, Lin W, Shen D. 2010. Neonatal brain image segmentation in longitudinal MRI studies. *Neuroimage.* 49:391–400.
- Shi Y, Lai R, Krishna S, Sicotte N, Dinov I, Toga AW. 2008. Anisotropic Laplace-Beltrami eigenmaps: bridging Reed graphs and skeletons. *Proc IEEE Comput Soc Conf Comput Vis Pattern Recognit.* 2008:1–7.
- Shi Y, Lai R, Morra JH, Dinov I, Thompson PM, Toga AW. 2010. Robust surface reconstruction via Laplace-Beltrami eigen-projection and boundary deformation. *IEEE Trans Med Imaging.* 29:2009–2022.
- Shi Y, Lai R, Wang DJJ, Pelletier D, Mohr D, Sicotte N, Toga AW. 2014. Metric optimization for surface analysis in the Laplace-Beltrami embedding space. *IEEE Trans Med Imaging.* 33:1447–1463.
- Shi Y, Morra J, Thompson P, Toga A. 2009. Inverse-consistent surface mapping with Laplace-Beltrami eigen-features. *Comp Imag Vis.* 21:467–478.
- Shi F, Wang L, Wu G, Li G, Gilmore JH, Lin W, Shen D. 2014. Neonatal atlas construction using sparse representation. *Hum Brain Mapp.* 35:4663–4677.
- Shi F, Yap PT, Fan Y, Gilmore JH, Lin W, Shen D. 2010. Construction of multi-region-multi-reference atlases for neonatal brain MRI segmentation. *Neuroimage.* 51:684–693.
- Shokouhi M, Barnes A, Suckling J, Moorhead TW, Brennan D, Job D, Lymer K, Dazzan P, Reis Marques T, MacKay C, et al. 2011. Assessment of the impact of the scanner-related factors on brain morphometry analysis with Brainvisa. *BMC Med Imaging.* 11:23.
- Shuter B, Yeh IB, Graham S, Au C, Wang SC. 2008. Reproducibility of brain tissue volumes in longitudinal studies: effects of changes in signal-to-noise ratio and scanner software. *Neuroimage.* 41:371–379.
- Smith SM, Jenkinson M, Woolrich MW, Beckmann CF, Behrens TEJ, Johansen-Berg H, Bannister PR, De Luca M, Drobnjak I, Flitney DE, et al. 2004. Advances in functional and structural MR image analysis and implementation as FSL. *Neuroimage.* 23:208–219.
- Smith DM, Mizumori SJY. 2006. Hippocampal place cells, context, and episodic memory. *Hippocampus.* 16:716–729.
- Sorrells SF, Paredes MF, Cebrian-silla A, Sandoval K, Qi D, Kevin W, James D, Mayer S, Chang J, Auguste KI, et al. 2018. Human hippocampal neurogenesis drops sharply in children to undetectable levels in adults. *Nature.* 555:377–381.
- Spalding KL, Bergmann O, Alkass K, Bernard S, Salehpour M, Huttner HB, Boström E, Westerlund I, Vial C, Buchholz BA, et al. 2013. Dynamics of hippocampal neurogenesis in adult humans. *Cell.* 153:1219–1227.
- Stokes J, Kyle C, Arne DE. 2015. Complementary roles of human hippocampal subfields in differentiation and integration of spatial context. *J Cogn Neurosci.* 27:546–559.
- Stonnington CM, Tan G, Klöppel S, Chu C, Draganski B, Jack CR, Chen K, Ashburner J, Frackowiak RSJ. 2008. Interpreting scan data acquired from multiple scanners: a study with Alzheimer's disease. *Neuroimage.* 39:1180–1185.

- Strange BA, Witter MP, Lein ES, Moser EI. 2014. Functional organization of the hippocampal longitudinal axis. *Nat Rev Neurosci.* 15:655–669.
- Sun J, Bonaguidi MA, Jun H, Guo JU, Sun GJ, Will B, Yang Z, Jang M-H, Song H, Ming G, et al. 2015. A septo-temporal molecular gradient of *sfrp3* in the dentate gyrus differentially regulates quiescent adult hippocampal neural stem cell activation. *Mol Brain.* 8:52.
- Takao H, Hayashi N, Ohtomo K. 2014. Effects of study design in multi-scanner voxel-based morphometry studies. *Neuroimage.* 84:133–140.
- Tavares RM, Mendelsohn A, Grossman Y, Shapiro M, Trope Y, Schiller D, Tavares RM, Mendelsohn A, Grossman Y, Williams CH, et al. 2015. A Map for Social Navigation in the Human Brain. *Neuron.* 87:231–243.
- Thompson PM, Hayashi KM, De Zubicaray GI, Janke AL, Rose SE, Semple J, Hong MS, Herman DH, Gravano D, Doddrell DM, et al. 2004. Mapping hippocampal and ventricular change in Alzheimer disease. *Neuroimage.* 22:1754–1766.
- Toda T, Parylak SL, Linker SB, Gage FH, Gage FH. 2018. The role of adult hippocampal neurogenesis in brain health and disease. *Mol Psychiatry.* doi:10.1038/s41380-018-0036-2.
- Uematsu A, Matsui M, Tanaka C, Takahashi T, Noguchi K, Suzuki M, Nishijo H. 2012. Developmental trajectories of amygdala and hippocampus from infancy to early adulthood in healthy individuals. *PLoS One.* 7:e46970.
- Voevodskaya O, Simmons A, Nordenskjöld R, Kullberg J, Ahlström H, Lind L, Wahlund L-O, Larsson E-M, Westman E, Initiative ADN. 2014. The effects of intracranial volume adjustment approaches on multiple regional MRI volumes in healthy aging and Alzheimer's disease. *Front Aging Neurosci.* 6:1–14.
- Voineskos AN, Winterburn JL, Felsky D, Pipitone J, Rajji TK, Mulsant BH, Chakravarty MM. 2015. Hippocampal (subfield) volume and shape in relation to cognitive performance across the adult lifespan. *Hum Brain Mapp.* 36:3020–3037.
- Wiggins GC, Triantafyllou C, Potthast A, Reykowski A, Nittka M, Wald LL. 2006. 32-Channel 3 tesla receive-only phased-array head coil with soccer-ball element geometry. *Magn Reson Med.* 56:216–223.
- Wilke M, Schmithorst VJ, Holland SK. 2002. Assessment of spatial normalization of whole-brain magnetic resonance images in children. *Hum Brain Mapp.* 17:48–60.
- Wilke M, Schmithorst VJ, Holland SK. 2003. Normative pediatric brain data for spatial normalization and segmentation differs from standard adult data. *Magn Reson Med.* 50:749–757.
- Williams L-A, Gelman N, Picot PA, Lee DS, Ewing JR, Han VK, Thompson RT. 2005. Neonatal brain: regional variability of in vivo MR imaging relaxation rates at 3.0 T—initial experience. *Radiology.* 235:595–603.
- Winterburn JL, Pruessner JC, Chavez S, Schira MM, Lobaugh NJ, Voineskos AN, Chakravarty MM. 2013. A novel in vivo atlas of human hippocampal subfields using high-resolution 3T magnetic resonance imaging. *Neuroimage.* 74:254–265.
- Wise PM. 2006. Estrogen therapy: does it help or hurt the adult and aging brain? Insights derived from animal models. *Neuroscience.* 138:831–835.
- Wisse LEM, Gerritsen L, Zwanenburg JJM, Kuijf HJ, Luijten PR, Biessels GJ, Geerlings MI. 2012. Subfields of the hippocampal formation at 7T MRI: in vivo volumetric assessment. *Neuroimage.* 61:1043–1049.
- Woo C-W, Krishnan A, Wager TD. 2014. Cluster-extent based thresholding in fMRI analyses: pitfalls and recommendations. *Neuroimage.* 91:412–419.
- Worsley KJ, Andermann M, Koulis T, MacDonald D, Evans AC. 1999. Detecting changes in nonisotropic images. *Hum Brain Mapp.* 8:89–101.
- Worsley KJ, Evans AC, Marrett S, Neelin P. 1992. A three-dimensional statistical analysis for CBF activation studies in human brain. *J Cereb Blood Flow Metab.* 12:900–918.
- Yoon U, Fonov VS, Perusse D, Evans AC. 2009. The effect of template choice on morphometric analysis of pediatric brain data. *Neuroimage.* 45:769–777.
- Yuen GS, McEwen BS, Akama KT. 2011. LIM kinase mediates estrogen action on the actin depolymerization factor Cofilin. *Brain Res.* 1379:44–52.
- Yurgelun-Todd DA, Killgore WDS, Cintron CB. 2003. Cognitive correlates of medial temporal lobe development across adolescence: a magnetic resonance imaging study. *Percept Mot Skills.* 96:3–17.
- Yushkevich PA, Amaral RSC, Augustinack JC, Bender AR, Bernstein JD, Boccardi M, Bocchetta M, Burggren AC, Carr VA, Chakravarty MM, et al, (HSG) for the HSG. 2015. Quantitative comparison of 21 protocols for labeling hippocampal subfields and parahippocampal subregions in in vivo MRI: towards a harmonized segmentation protocol. *Neuroimage.* 111:526–541.
- Yushkevich PA, Pluta JB, Wang H, Xie L, Ding SL, Gertje EC, Mancuso L, Kliot D, Das SR, Wolk DA. 2015. Automated volumetry and regional thickness analysis of hippocampal subfields and medial temporal cortical structures in mild cognitive impairment. *Hum Brain Mapp.* 36:258–287.
- Zeidman P, Lutti A, Maguire EA. 2015. Investigating the functions of subregions within anterior hippocampus. *Cortex.* 73:240–256.
- Zeineh MM, Palomero-Gallagher N, Axer M, Gräpel D, Goubran M, Wree A, Woods R, Amunts K, Zilles K. 2017. Direct visualization and mapping of the spatial course of fiber tracts at microscopic resolution in the human hippocampus. *Cereb Cortex.* 27:1779–1794.
- Østby Y, Tamnes CK, Fjell AM, Westlye LT, Due-Tønnessen P, Walhovd KB. 2009. Heterogeneity in subcortical brain development: a structural magnetic resonance imaging study of brain maturation from 8 to 30 years. *J Neurosci.* 29:11772–11782.